*Proceedings of the 2nd International Conference on Computational Heat and Mass Transfer*
COPPE/EE/UFRJ – Federal University of Rio de Janeiro, Brazil, October 22-26, 2001

# STRICT IMPLEMENTATION OF LYAPUNOV FUNCTIONAL AND PATTERN ANALYSIS IN SWIFT-HOHENBERG NONUNIFORMLY FORCED DYNAMICS

JOSÉ PONTES*, C. I. CHRISTOV†, R. R. ROSA‡, F. M. RAMOS§, C. RODRIGUES NETO¶, AND E. L. REMPEL‖

**Abstract.** Using the operator-splitting method Christov & Pontes (2000, 2001) developed a second-order in time implicit difference scheme for solving the Swift-Hohenberg equation (S-H) which describes pattern formation in Rayleigh-Benard cells. For each time step the scheme involves internal iterations which improve the stability and increase the accuracy with which the Lyapunov functional for S-H is approximated. Different cases of pattern formation were treated and it was shown that the new scheme reaches the stationary pattern several times faster than the previously used first-order in time schemes. In this work we review the main steps concerning the derivation of the second-order in time scheme the demonstration that the scheme strictly satisfies a discrete approximation of the Lyapunov functional. Results of numerical simulations conducted in three large boxes with nonuniform forcings across the box are presented, illustrating that this scheme preserves the non-increasing time-dependent behaviour of the functional. The results are compared with a simulation conducted in a uniformly forced system. The rate of change of the functional is generaly slow save the pecipituous downfalls during the time intervals in which the pattern changes qualitatively.

Keywords: Nonlinear Systems, Bénard Convection, Implicit Methods, Finite Difference Methods

**1. Introduction.** A widely accepted model for the thermal convection in a thin layer of fluid heated from below is the so-called Swift-Hohenberg equation (SH, for breivity) (Swift & Hohenberg, 1977) which is a nonlinear parabolic equations containing fourth-order space-derivatives (generalized diffusion equation). It describes the pattern formation in fluid layers confined between horizontal well-conducting boundaries.

Unlike the models that describe wave propagation on the surface of convective layer, the SH equation possesses a Lyapunov functional which ensures the potential behaviour of the solution. Among other properties of the potential evolution is that one cannot have spatio-temporal chaos, but only spatial one. However, if one uses a difference scheme which does not faithfully represent the Lyapunov functional one might encounter numerically some non-physical effects. For instance, when the Lyapunov functional is only approximately enforced, then initially the solution approaches one of the attractors in the functional space but eventually leaves the domain of attraction of that particular steady-state solution after being "kicked" from one of the small disturbances the latter arising from the inadequate approximation. Then the solution may keep wandering between several of the attractors exhibiting spatio-temporal chaotic behavior which is not possible for the original model.

Solving SH numerically is a challenge because of the interplay between the higher-order diffusion (higher-order spatial derivatives) and nonlinearity on the one hand, and the presence of a Lyapunov functional – on the other. A computationally efficient difference scheme for SH was developed by Christov et al (1997) where a first-order in time implicit time-stepping is used in the framework of the operator-splitting methods.

There are very few papers in the literature which deal with the problems connected to the numerical implementation of an additional integral constraint on the solution, such as the Lyapunov functional. For the case of Lyapunov constraint in a conservative system (such as Nonlinear Schrödinger equation) one is referred to the work of Ivonin (1999). Though some fine approximations of the additional integral constraint are presented in the above mentioned papers, they are not in fact strictly preserving approximations. We believe, the strict implementation is crucial if one is to deal with more complex models.

* Metallurgy and Materials Engineering Dept – EE/COPPE/UFRJ, PO Box 68505, 21945-970 Rio de Janeiro RJ, Brazil jopontes@ufrj.br

† Dept. of Mathematics, University of Louisiana at Lafayette, Lafayette, LA 70504-1010 christov@louisiana.edu

‡ LAC-INPE P. O. Box 515 12201-970, S. José dos Campos, SP, Brazil reinaldo@lac.inpe.br

§ LAC-INPE P. O. Box 515 12201-970, S. José dos Campos, SP, Brazil fernando@lac.inpe.br

¶ LAC-INPE P. O. Box 515 12201-970, S. José dos Campos, SP, Brazil camilo@lac.inpe.br

‖ LAC-INPE P. O. Box 515 12201-970, S. José dos Campos, SP, Brazil erico@lac.inpe.br

In this work we review the main steps concerning the derivation of the second-order in time scheme and prove that the scheme strictly satisfies a discrete approximation of the Lyapunov functional (see also Christov & Pontes 2000, 2001). The scheme employs internal iterations to secure adequate approximation of the nonlinear term. Results of numerical simulations conducted in four large boxes are presented, illustrating that this scheme preserves the non-increasing time-dependent behaviour of the functional.

**2. Posing the Problem.** Consider a rectangular region $D : \{x \in [0, L_x,],\ y \in [0, L_y]\}$ with boundary $\partial D$ at which different types of b.c. can be imposed. Consider the following Generalized Diffusion Equation (GDE):

$$\frac{\partial u}{\partial t} = -D(\Delta + \kappa^2)^2 + F(u) \equiv -D\Delta\Delta u - 2D\kappa^2\Delta u - D\kappa^4 + F(u)\,. \tag{2.1}$$

For the cubic nonlinearity one has the following potential function

$$F(u) = -\frac{dU(u)}{du} = \varepsilon(x)u - gu^3\,, \quad U(u) = -\frac{\varepsilon(x)}{2}u^2 + \frac{g}{4}u^4\,. \tag{2.2}$$

Eq.(2.1) with (2.2) acknowledged is the Swift-Hohenberg equation (SH, for brevity) derived for the Rayleigh-Bénard convection to account for the formation of convective rolls in high Prandtl number fluid layers. The variable $u(x, y, t)$ describes the horizontal planform of the temperature deviation from the conductive profile.

The correct set of lateral b.c. is the one which secures that the evolution of the "energy" $\int v^2$ depends only on its production or dissipation in the bulk, but not on the surface. In other words, in the balance equation for the evolution of energy

$$\frac{d}{dt}\frac{1}{2}\int_D v^2 dxdy = -\oint_{\partial D} v\frac{\partial a_4(x,y,t)\Delta v}{\partial n}\mathrm{d}l - \oint_{\partial D} a_4(x,y,t)\Delta v\frac{\partial v}{\partial n}\mathrm{d}l - \oint_{\partial D} a_2(x,y,t)v\frac{\partial v}{\partial n}\mathrm{d}l -$$
$$\int_D a_0(x,y,t)(\Delta v)^2\mathrm{d}x\mathrm{d}y - \int_D a_2(x,y,t)(\nabla v)^2\mathrm{d}x\mathrm{d}y - \int_D a_0(x,y,t)v^2\mathrm{d}x\mathrm{d}y$$

one has to make the surface integrals vanish. This can happen if one of the following admissible b.c. conditions are imposed

$$v = \frac{\partial v}{\partial n} = 0\,, \quad v = \Delta v = 0\,, \quad \frac{\partial v}{\partial n} = \frac{\partial \Delta v}{\partial n} = 0\,, \qquad (x, y) \in \partial D, \tag{2.3}$$

where $n$ stands for the outward normal direction to the boundary $\partial D$. We call $(2.3)_1$ and $(2.3)_2$ "generalized Dirichlet conditions" of the first and second kind, respectively. The condition $(2.3)_3$ involves only derivatives at the boundary, hence the coinage – "generalized Neumann condition".

The main feature of (2.1) is that the damping of perturbations occurs via the fourth-order spatial derivatives, while the term with second-order spatial derivatives enhances the perturbations. This allows the occurrence of a linear bifurcation of the solution for certain values of the parameters and/or the size of domain. The nontrivial solutions branch out from a (generally motionless) reference state. Their shapes are the result of the interplay between the complicated linear operator and the nonlinearity. From the perspective of GDE it is clear that a bifurcation can take place only for sufficiently large domains whose size is commensurate with the length scales of the patterns.

SH admits a non-increasing Lyapunov functional

$$\Psi = \int_D \left\{ -\frac{\varepsilon}{2}u^2 + \frac{g}{4}u^4 + \frac{D}{2}\left[(\Delta u)^2 - 2\kappa^2(\nabla u)^2 + \kappa^4 u^2\right] \right\} \mathrm{d}x\,\mathrm{d}y, \tag{2.4}$$

$$\frac{\partial \Psi}{\partial t} = -\int_D \left(\frac{\partial u}{\partial t}\right)^2 \mathrm{d}x\,\mathrm{d}y < 0\,, \tag{2.5}$$

which rules out the complex temporal or spatio-temporal behavior in the long time (turbulent, oscillatory, or chaotic) and allows formation of steady convective patterns. In their turn these steady patterns can be quite complicated in shape, e.g., spatially chaotic.

Consider the rectangle $x \in [0, L_x]$, $y \in [0, L_y]$ and the Dirichlet b.c. of the first and second kind:

$$u = \frac{\partial u}{\partial x} = 0 \text{ for } x = 0,\ L_x; \qquad u = \frac{\partial u}{\partial y} = 0 \text{ for } y = 0,\ L_y, \tag{2.6}$$

$$u = \frac{\partial^2 u}{\partial x^2} = 0 \text{ for } x = 0,\ L_x; \qquad u = \frac{\partial^2 u}{\partial y^2} = 0 \text{ for } y = 0,\ L_y, \tag{2.7}$$

Respectively, the Neumann condition is

$$\frac{\partial u}{\partial x} = \frac{\partial^2 u}{\partial x^2} = 0 \quad \text{for} \quad x = 0,\ L_x, \qquad \frac{\partial u}{\partial y} = \frac{\partial^2 u}{\partial y^2} = 0 \quad \text{for} \quad y = 0,\ L_y, \tag{2.8}$$

There is no restriction to use mixed types of b.c. which are combinations of Dirichlet and Neumann conditions. If the scheme and algorithm perform properly for the "pure" cases (including the Neumann one), then they will do the same for the mixed cases, since any admissible (in the sense of (2.3)) mixture of boundary conditions yields a well posed boundary value problem. For the sake of simplicity we restrict ourselves in the present work to Dirichlet conditions of the first kind.

**3. Difference Scheme.**

**3.1. Implicit Time-Stepping.** It is not possible to achieve a strict satisfaction of a discrete version of the Lyapunov functional with an explicit scheme which has only two time stages (levels). On the other hand, it is not obvious how the problem can be solved through using multi-level scheme. It is *a-priori* clear that a scheme which is both implicit in time and nonlinear will possess the necessary symmetry to accommodate for the existence of a non-increasing functional. The key to the scheme which satisfies the additional integral constraint (the Lyapunov functional) is the approximation of the nonlinear potential term. A scheme for (2.1) which is implicit and nonlinear reads

$$\frac{u^{n+1}-u^n}{\tau} = D\left[-\frac{\partial^4}{\partial x^4} - \frac{\partial^4}{\partial y^4} - 2k^2\frac{\partial^2}{\partial x^2} - 2k^2\frac{\partial^2}{\partial y^2} - 2\frac{\partial^4}{\partial x^2 \partial y^2} - k^4\right]\frac{u^{n+1}+u^n}{2} - \frac{U(u^{n+1})-U(u^n)}{u^{n+1}-u^n}, \tag{3.1}$$

where $U(u)$ stands for the potential of the nonlinear force acting upon the system. For the particular case of quartic potential the nonlinear term adopts the form:

$$-\frac{U(u^{n+1})-U(u^n)}{u^{n+1}-u^n} = \frac{\varepsilon(x)}{2}[u^{n+1}+u^n] - \frac{g}{4}\left[(u^{n+1})^3 + (u^{n+1})^2 u^n + u^{n+1}(u^n)^2 + (u^n)^3\right].$$

**3.2. Internal Iterations.** The scheme (3.1) is nonlinear and can be solved only by means of iterating the solution within a given time step. Additional benefit from the iterations is that they allow us to alleviate a possible problem connected with the inversion of the linear operators when they are not negative definite. This kind of complications can be expected only when $max\{L_x, L_y\}k_0 \geq \alpha$, where $\alpha$ can be estimated from the inclusion theorem. As already mentioned, a simple consequence of the non-definiteness of the linear operator is the occurrence of a linear bifurcation of the stationary problem. We tackle this complication by means of an explicit approximation of the second-order terms. Thus the iterative scheme reads

$$\frac{u^{n,k+1}-u^n}{\tau} = \left[-D\frac{\partial^4}{\partial x^4} - D\frac{\partial^4}{\partial y^4} - Dk^4\right]\frac{u^{n,k+1}+u^n}{2} + \left[-2Dk^2\frac{\partial^2}{\partial x^2} - 2Dk^2\frac{\partial^2}{\partial y^2} - 2D\frac{\partial^4}{\partial x^2 \partial y^2} + \varepsilon(x)\right]\frac{u^{n,k}+u^n}{2} - \frac{g}{4}\left[(u^{n,k})^2 + u^{n,k}u^n + (u^n)^2\right]u^{n,k+1} - \frac{g}{4}(u^n)^3. \tag{3.2}$$

Here the superscript $(n, k+1)$ designates the current ("new") iteration of the unknown set function while the indices $(n, k)$ and $(n)$ distinguish the quantities known from the previous iteration and the previous time step, respectively. The scheme with internal iterations is linear for $u^{n,k+1}$. The internal iterations are conducted until the following criterion is satisfied

$$\frac{\max\|u^{n,K+1} - u^{n,K}\|}{\max\|u^{n,K+1}\|} < \delta, \tag{3.3}$$

for certain $k = K$. Then the last iteration gives the sought function on the new time stage, $u^{n+1} \stackrel{\text{def}}{=} u^{n,K+1}$.

The gist of the concept of internal iterations is that the same time step is repeated until convergence. Since the iterative process begins from an initial condition which is the value of the sought function from the previous time step, the number of internal iterations needed for convergence depends heavily on the magnitude of the time increment $\tau$. For smaller $\tau$ the initial condition for the iterations is closer to the

sought function and the number of iterations is expected to be small. The trade-off is that a very small $\tau$ requires a larger number of time steps which increases the overall number of arithmetic operations per nodal point. Conversely, an inappropriately large $\tau$ will bring about a larger number of internal iterations per time step increasing significantly the computational time needed to achieve a single time step dispelling thus the advantage of the larger "strides" (the faster time-stepping). The dependence of the number of internal iterations on $\tau$ is nonlinear and leaves a room for optimization. Our numerical experiments show that the calculations are cost effective if the number of internal iterations is in the interval $4 \leq K \leq 16$. This estimate calls for a reduction of the time step when faster processes are treated for which the evolution from a given time stage to the next time stage involves a significant deformation of the field. This means that when faster temporal transients are involved, the usage of larger time steps $\tau$ leading to $K \gg 20$ is not justified regardless to the fact that formally speaking the implicit scheme is still stable.

**3.3. The Splitting.** The inversion of the matrix of Eq. (3.2) is a rather costly procedure even though it is sparse. The 3D case is drastically more expensive. Moreover that the internal iterations require the process to be repeated several times during each time step. Then it is only natural to introduce operator splitting in order to minimize the operations per unit iteration and hence per one time step.

We settle here for the *second Douglas scheme* (Douglas, 1956) (also called "scheme of stabilizing correction" (Yanenko, 1971) which gives the full-time-step approximation for non-commutative operators and is more robust for nonlinear problems than ADI (see Yanenko, 1971) for a review of the splitting schemes and strategies). Another advantage of the stabilizing correction is that for linear problems in 3D it is absolutely stable, while ADI is not. We generalize the Douglas scheme for fourth-order operators and modify it to be second order accurate in time (a Crank-Nicolson type of scheme) as follows

$$\frac{\tilde{u}-u^n}{\tau} = L_{11}^{n,k}\tilde{u} + L_{22}^{n,k}u^n + \frac{1}{2}\left[-D\frac{\partial^4}{\partial x^4} - D\frac{\partial^4}{\partial y^4} - Dk^4 + \frac{g}{2}\left(u^n\right)^2\right]u^n + \frac{1}{2}\left[-L_{12}-L_1-L_2\right]\left[u^{n,k}+u^n\right]$$

$$\frac{u^{n,k+1}-\tilde{u}}{\tau} = L_2^{n,k}(u^{n,k+1}-u^n)$$

where

$$L_{11}^{n,k} \stackrel{\text{def}}{=} -\frac{D}{2}\frac{\partial^4}{\partial x^4} - \frac{D}{4}k^4 + \frac{g}{8}\left[\left(u^{n,k}\right)^2 + u^{n,k}u^n + \left(u^n\right)^2\right] \tag{3.4}$$

$$L_{22}^{n,k} \stackrel{\text{def}}{=} -\frac{D}{2}\frac{\partial^4}{\partial y^4} - \frac{D}{4}k^4 + \frac{g}{8}\left[\left(u^{n,k}\right)^2 + u^{n,k}u^n + \left(u^n\right)^2\right] + \frac{\varepsilon(x)}{2} \tag{3.5}$$

$$L_{12} \stackrel{\text{def}}{=} 2D\frac{\partial^4}{\partial x^2\partial y^2}, \qquad L_1 \stackrel{\text{def}}{=} 2Dk^2\frac{\partial^2}{\partial x^2} + \frac{\varepsilon(x)}{2}, \qquad L_2 \stackrel{\text{def}}{=} 2Dk^2\frac{\partial^2}{\partial y^2} + \frac{\varepsilon(x)}{2} \tag{3.6}$$

Christov *et al* (2001) showed that the splitting scheme approximates the desired scheme in full-time steps within the adopted order of approximation $O(\tau^2)$. This demonstration will not be repeated here. Thus, employing a splitting does not degrade the temporal approximation of the scheme. In other words, the splitting scheme coincides with the original scheme within the order of approximation of the latter.

**4. Implementation of the Lyapunov Functional.** After the iterations converge one has $u^{n+1} = u^{n,k+1} = u^{n,k}$ and hence one arrives at a nonlinear scheme in full-time steps which is exactly the difference approximation of scheme (3.1) when in the latter the operators $L$ are replaced by their standard second-order representations in finite differences, $\Lambda$ (see Christov et al, 1997), namely

$$\frac{u^{n+1}-u^n}{\tau} = (\Lambda_{11}+\Lambda_{22}-\Lambda_1-\Lambda_2+2\Lambda_{12})\frac{u^{n+1}+u^n}{2} + \frac{U(u^{n+1})-U(u^n)}{u^{n+1}-u^n}\,, \tag{4.1}$$

where

$$\frac{U(u^{n+1})-U(u^n)}{u^{n+1}-u^n} = -\frac{\varepsilon}{2}\left[u^{n+1}+u^n\right] + \frac{g}{4}\left[(u^{n+1})^3 + (u^{n+1})^2u^n + u^{n+1}(u^n)^2 + (u^n)^3\right].$$

Note that in the left-hand side we neglected the $O(\tau^2)$ contribution to the operator $B$ as asymptotically vanishing with respect to unity (See also Christov and Pontes 2001).

Upon multiplying eq.(4.1) by $(u_{ij}^{n+1}-u_{ij}^{n})/\tau$ and taking the sum over the spatial indices one obtains

$$\sum_{i=2}^{M-1}\sum_{j=2}^{N-1}\left[\frac{u_{i,j}^{n+1}-u_{i,j}^{n}}{\tau}\right]^2=\sum_{i=2}^{M-1}\sum_{j=2}^{N-1}\left\{\frac{\varepsilon}{2\tau}\left[\left(u_{i,j}^{n+1}\right)^2-\left(u_{i,j}^{n}\right)^2\right]-\frac{g}{4\tau}\left[\left(u_{i,j}^{n+1}\right)^4-\left(u_{i,j}^{n}\right)^4\right]\right\}$$
$$+\sum_{i=2}^{M-1}\sum_{j=2}^{N-1}\frac{u_{i,j}^{n+1}-u_{i,j}^{n}}{\tau}[\Lambda_{11}+\Lambda_{22}-\Lambda_1-\Lambda_2+2\Lambda_{12}]\frac{u_{i,j}^{n+1}+u_{i,j}^{n}}{2} \tag{4.2}$$

The last term is manipulated using integration (summation) by parts and the discrete form of boundary conditions for $u$ (2.6), (2.7) are acknowledged. We demonstrate the procedure on the difference operators in $x$-direction and for $\Lambda_{11}$ we get

$$\frac{1}{2\tau}\sum_{i=2}^{M-1}u_{ij}^{n+1}\Lambda_{11}u_{i,j}^{n+1}\stackrel{\text{def}}{=}-\frac{D}{2h_x^4\tau}\sum_{i=2}^{M-1}u_{ij}^{n+1}\left[u_{i-2,j}^{n+1}-4u_{i-1,j}^{n+1}+6u_{i,j}^{n+1}-4u_{i+1,j}^{n+1}+u_{i+2,j}^{n+1}\right]$$
$$\equiv-\frac{D}{2h_x^4\tau}\sum_{i=3}^{M-2}u_{ij}^{n+1}\left[u_{i-2,j}^{n+1}-4u_{i-1,j}^{n+1}+6u_{i,j}^{n+1}-4u_{i+1,j}^{n+1}+u_{i+2,j}^{n+1}\right]$$
$$=-\frac{D}{2h_x^4\tau}\sum_{i=2}^{M-1}\left[2u_{i+1,j}^{n+1}u_{i-1,j}^{n+1}-4u_{i-1,j}^{n+1}u_{i,j}^{n+1}+6u_{i,j}^{n+1}u_{i,j}^{n+1}-4u_{i+1,j}^{n+1}u_{i,j}^{n+1}\right]$$
$$-\frac{D}{2h_x^4\tau}\left[-u_{Mj}^{n+1}u_{M-2j}^{n+1}-u_{M-1j}^{n+1}u_{M-3j}^{n+1}-u_{4j}^{n+1}u_{2j}^{n+1}-u_{3j}^{n+1}u_{1j}^{n+1}\right]$$
$$-\frac{D}{2h_x^4\tau}\left[4u_{Mj}^{n+1}u_{M-1j}^{n+1}+4u_{M-1j}^{n+1}u_{M-2j}^{n+1}+4u_{3j}^{n+1}u_{2j}^{n+1}+4u_{2j}^{n+1}u_{1j}^{n+1}\right]$$
$$-\frac{D}{2h_x^4\tau}\left[-6\left(u_{M-1j}^{n+1}\right)^2-6\left(u_{2j}^{n+1}\right)^2\right]=-\frac{D}{2\tau}\sum_{i=2}^{M-1}\left[\frac{u_{i+1,j}^{n+1}-2u_{i,j}^{n+1}+u_{i-1,j}^{n+1}}{h_x^2}\right]^2 \tag{4.3}$$

Similarly for $\Lambda_1$

$$-\frac{1}{2\tau}\sum_{i=2}^{M-1}u_{ij}^{n+1}\Lambda_1u_{i,j}^{n+1}\stackrel{\text{def}}{=}-\frac{2Dk^2}{2h_x^2\tau}\sum_{i=2}^{M-1}u_{ij}^{n+1}\left[u_{i-1,j}^{n+1}-2u_{i,j}^{n+1}+u_{i+1,j}^{n+1}\right]$$
$$=-\frac{2Dk^2}{2h_x^2\tau}\left\{\sum_{i=2}^{M-1}\left[u_{i,j}^{n+1}u_{i+1,j}^{n+1}-\frac{1}{2}\left(u_{i+1,j}^{n+1}\right)^2-\frac{1}{2}\left(u_{i,j}^{n+1}\right)^2\right]+\frac{1}{2}\left[\left(u_2^{n+1}j\right)^2-\left(u_{Mj}^{n+1}\right)^2\right]\right\}$$
$$-\frac{2Dk^2}{2h_x^2\tau}\left\{\sum_{i=2}^{M-1}\left[u_{ij}^{n+1}u_{i-1,j}^{n+1}-\frac{1}{2}\left(u_{i,j}^{n+1}\right)^2-\frac{1}{2}\left(u_{i-1,j}^{n+1}\right)^2\right]-\frac{1}{2}\left[\left(u_1^{n+1}j\right)^2+\left(u_{M-1j}^{n+1}\right)^2\right]\right\}$$
$$=\frac{2Dk^2}{4\tau}\sum_{i=2}^{M-1}\left\{\left[\frac{u_{i+1,j}^{n+1}-u_{i,j}^{n+1}}{h_x}\right]^2+\left[\frac{u_{i,j}^{n+1}-u_{i-1,j}^{n+1}}{h_x}\right]^2\right\} \tag{4.4}$$

Making use of the same technique on can show that

$$\frac{1}{2\tau}\sum_{i=2}^{M-1}u_{ij}^{n}\Lambda_{11}u_{i,j}^{n+1}-u_{ij}^{n+1}\Lambda_{11}u_{i,j}^{n}=0,\qquad\frac{1}{2\tau}\sum_{j=2}^{N-1}u_{ij}^{n}\Lambda_{22}u_{i,j}^{n+1}-u_{ij}^{n+1}\Lambda_{22}u_{i,j}^{n}=0,$$
$$\frac{1}{2\tau}\sum_{i=2}^{M-1}u_{ij}^{n}\Lambda_{1}u_{i,j}^{n+1}-u_{ij}^{n+1}\Lambda_{1}u_{i,j}^{n}=0,\qquad\frac{1}{2\tau}\sum_{j=2}^{N-1}u_{ij}^{n}\Lambda_{2}u_{i,j}^{n+1}-u_{ij}^{n+1}\Lambda_{2}u_{i,j}^{n}=0.$$

In the same vein are treated the terms connected with the $y$ spatial derivative. The approximation of the mixed fourth derivative make use of the above derivations in both $x$- and $y$-direction. We denote

$$\Phi_{ij}=\frac{u_{i,j-1}-2u_{ij}+u_{ij+1}}{h_y^2}.$$

Then

$$\sum_{i=2}^{M-1} u_{ij}\frac{\Phi_{i-1,j}-2\Phi_{ij}+\Phi_{i+1j}}{h_x^2}=\sum_{i=2}^{M-1}\Phi_{ij}\frac{u_{i-1,j}-2u_{ij}+u_{i+1j}}{h_x^2}$$
$$+\frac{u_{M-1j}\Phi_{Mj}-u_{1j}\Phi_{2j}}{h_x^2}+\frac{u_{Mj}\Phi_{M-1j}-u_{2j}\Phi_{1j}}{h_x^2}\equiv\sum_{i=2}^{M-1}\Phi_{ij}\frac{u_{i-1,j}-2u_{ij}+u_{i+1j}}{h_x^2},$$

and hence

$$2\sum_{i=2}^{M-1}\sum_{j=2}^{N-1}u_{ij}\Lambda_{12}u_{ij}=2\sum_{i=2}^{M-1}\sum_{j=2}^{N-1}\frac{u_{i-1,j}-2u_{ij}+u_{i+1j}}{h_x^2}\cdot\frac{u_{i,j-1}-2u_{ij}+u_{ij+1}}{h_y^2}$$

Now it is readily shown that the right-hand side of (4.2) is the time difference of the Lyapunov functional $\Psi$

$$\frac{\Psi^{n+1}-\Psi^n}{\tau}=-\sum_{i=2}^{M-1}\sum_{j=2}^{N-1}\left(\frac{u_{i,j}^{n+1}-u_{i,j}^n}{\tau}\right)^2 \tag{4.5}$$

$$\Psi^n=\sum_{i=2}^{M-1}\sum_{j=2}^{N-1}\left[-\frac{\varepsilon}{2}\left(u_{i,j}^n\right)^2+\frac{g}{4}\left(u_{i,j}^n\right)^4+\frac{Dk^4}{2}\left(u_{i,j}^n\right)^2\right]-\frac{2Dk^2}{4}\sum_{i=2}^{M-1}\sum_{j=2}^{N-1}\left[\frac{u_{i+1,j}^n-u_{i,j}^n}{h_x}\right]^2+\left[\frac{u_{i,j}^n-u_{i-1,j}^n}{h_x}\right]^2$$
$$+\left[\frac{u_{i,j+1}^n-u_{i,j}^n}{h_y}\right]^2+\left[\frac{u_{i,j}^n-u_{i,j-1}^n}{h_y}\right]^2+\frac{D}{2}\sum_{i=2}^{M-1}\sum_{j=2}^{N-1}\left[\frac{u_{i+1,j}^n-2u_{i,j}^n+u_{i-1,j}^n}{h_x^2}+\frac{u_{i,j+1}^n-2u_{i,j}^n+u_{i,j-1}^n}{h_y^2}\right]^2$$

The last formula presents a $O(\tau^2+h_x^2+h_y^2)$ approximation to the original Lyapunov functional (2.5) for the differential equation. The important point about difference version of the Lyapunov functional (4.5) is that it is strictly enforced provided that the internal iterations converge. Its satisfaction does not depend on the truncation error.

**5. Numerical Results.** The main subject of the present work is to demonstrate the impact of the implementation of the Lyapunov functional on the numerical dynamics. As featuring examples we consider four situatiuons: two systems forced with a bifurcation parameter which varies linearly along the direction parallel to one of the sidewalls. The third case comprises a system forced with a gaussian distribution of epsilon, the sidewalls being kept at an undercritical level. The fourth case consists of an uniformly forced configuration.

Before all we should mention that we checked the spatial and temporal discretizations on a simple case when the whole domain of the flow is occupied by a single convective cell. All mandatory tests involving doubling the temporal and spatial resolutions confirmed the second-order approximation of the scheme and the discrete implementation of the Lyapunov functional. The convergence of the internal iterations is tested for different values of the tolerance $\delta$ defined in eq. (3.3). The quantitative differences between the patterns are negligible for $\delta\leq 10^{-5}$. This allows us to choose $\delta=10^{-6}$.

In this work we present the results of four numrical simulations conducted in a box with size $L_x=50$ and $L_y=50$, with a spatial grid containing $302\times 302$ points (Figure 6.1 was run in a $30\times 30$ box with a mess containg $302\times 302$ points. The first two simulations were conducted with a forcing $\varepsilon=0.25$ and two different random initial conditions whereas we adopted $\varepsilon=0.5$ in the other two and same initial conditions used in the former ones. The results of these four simulations are summarized in Figs. (5.1) and (6.1).

For the sake of definiteness and backward compatibility with the works from the literature we select $\kappa_0=3.1172$, $g=12.9$, and $D=0.015$ which values correspond to a typical Rayleigh-Bénard convection with pattern formation (see, e.g. Swift & Hohenberg, 1977). When the size of the box is $L_x=L_y=50$, the selected value for $k_0$ allows roughly 50 convective cells in each direction. A staggered mesh with $302\times 302$ points is used which gives a spatial resolution of approximately 6 points per convective cell (12 points per wavelength). The time step used in all simulations was $\tau=0.02$.

The random initial condition is constructed by means of a random generator. The value of $u$ in the first point (lower-left corner) is calculated with the random generator for a given initial seed and then the rest if the grid points are filled row-wise using the previous point as a seed for the next point. Finally,

the initial field is renormalized to [-1,1]. Thus, the pattern can be referred by the number of the initial seed. We assess the rate of evolution of the pattern during the simulation by monitoring the relative $L_1$ norm defined as

$$L_1 = \frac{1}{\tau} \frac{\sum_{i,j} |u_{i,j}^{n+1} - u_{i,j}^{n}|}{\sum_{i,j} |u^{n+1}|}, \tag{5.1}$$

which roughly corresponds to the ratio between the spatial average of the modulus of time derivative $u_t$ and the spatial average of the modulus of the function itself.

The calculations begin from the random initial condition and proceeded until $L_1 \leq 5 \times 10^{-7}$ (except simulation shown in Fig. 6.1a), when it can be assumed that the motion is virtually steady. In all simulations the Lyapunov functional $\Psi(t)$ and $L_1$ rapidly decrease at the very beginning of the evolution. In this stage most of the spectral content of the random initial condition is filtered and only wavelengths close to $\kappa_0$ survive. The second stage is characterized by elimination of defects, resulting in longer correlation lenghts. The *phase* of the patterns evolve with minor changes in the average amplitude. The Lyapunov functional decreases at a much lower rate and $L_1$ norm evolves slower. However, the evolution of $L_1$ is not monotonical and accelerates when defects collapse. This behaviour is precisely captured by the sudden increases of the norm $L_1(t)$ and abrupt decreases in the Lyapunov functional.

We monitored also the number of internal iterations. In the time intervals of slow evolution, the number of internal iterations is around 1-3 in simulations made with internal precision $10^{-6}$ (Figs.5.1a,b and 6.1b). By specifying a higher precision the number of internal iterations per step rapidly increases, as shown in Figs.6.1a.

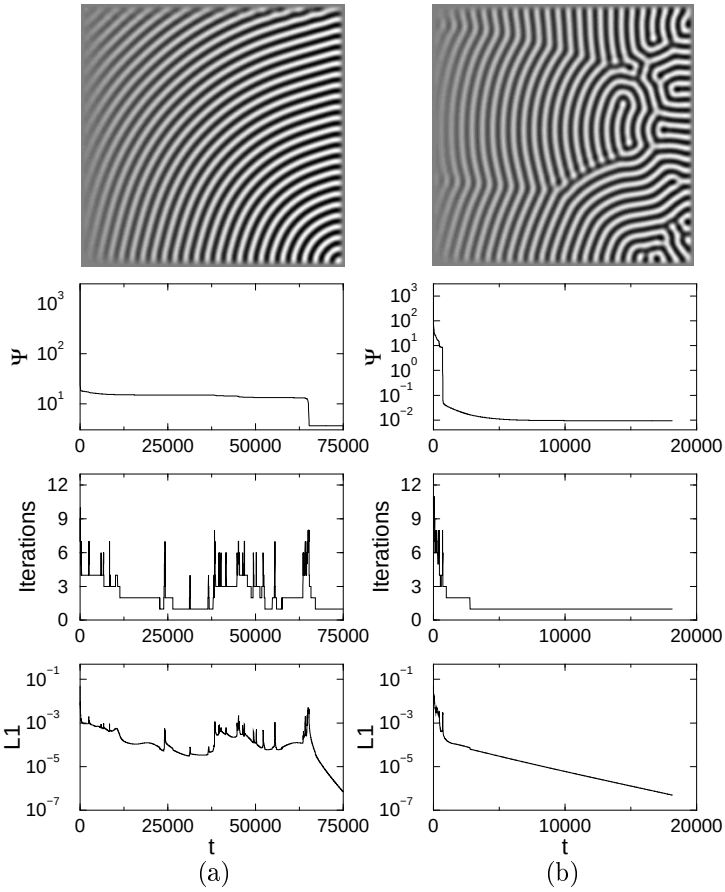


FIGURE 5.1. *Results obtained in two simulations run in a* $50 \times 50$ *box with a bifurcation parameter varying linearly along the horizontal sidewalls. Case (a): $\varepsilon$ varies from 0 at the left sidewall to 0.50 at right one. Case (b): $\varepsilon$ varies from 0 to 1.0. This figure shows the steady-state patterns, the time evolution of the associated Lyapunov finctional, the number of internal iterations accoplished in each time step and time evolution of* $L_1$. *Specified precision for the internal iterations:* $10^{-6}$. *Random initial condition seeds were generated in an IBM SP2 RISC 6000 using the* random *function and seed 123456.*

The simulations confirm the tendency of the rolls to align with a wall at which the bifurcation parameter is zero or negative, as can be seen in Figs. (5.1–6.1). The effect of increasing the forcing $\varepsilon$ applied to the system is also shown in the figures higher forcings lead to a higher density of defects and shorter correlation lengths due to the fact that a wider band of wavelengths becames linealy unstable. On the other hand the system forced with a gaussian distribution of $\varepsilon$ shows a lower level of *defects*, when compared with the other cases.

**6. Conclusions.** In the present work we review and applied the operator-splitting difference scheme proposed by Christov and Pontes (2000, 2001), for the numerical solution of nonlinear diffusion equations containing fourth-order space-derivatives. The scheme is of second-order approximation both in time and space and does not contain artificial dispersion, hence the disturbances are quickly attenuated. It is fully implicit owing to the use of internal iterations. The main characteristic of the scheme is that a discrete version of the Lyapunov functional which holds for the original quation is strictly implemented.

The performance of the scheme is demonstrated for the evolution of the solution of the Swift-Hohenberg (SH) equation in four simulations conducted in large boxes with two forcing levels and two different random initial conditions. The SH equation models the Rayleigh-Bénard convection in a horizontal layer. The strict implementation of the Lyapunov functional with its non-increasing behaviour is clearly demonstrated. The numerically obtained Lyapunov functional decreases more rapidly when the pattern undergoes qualitative changes (when the solution enters the immediate vicinity of the respective attractor). In all cases the evolution ended up in a spatially chaotic pattern. No temporal chaos was possible due to the strict satisfaction of the Lyapunov functional.

The proposed difference scheme can serve as a model for constructing approximations to nonlinear physical system when additional constraints, such as Lyapunov functional, are imposed on the solution.

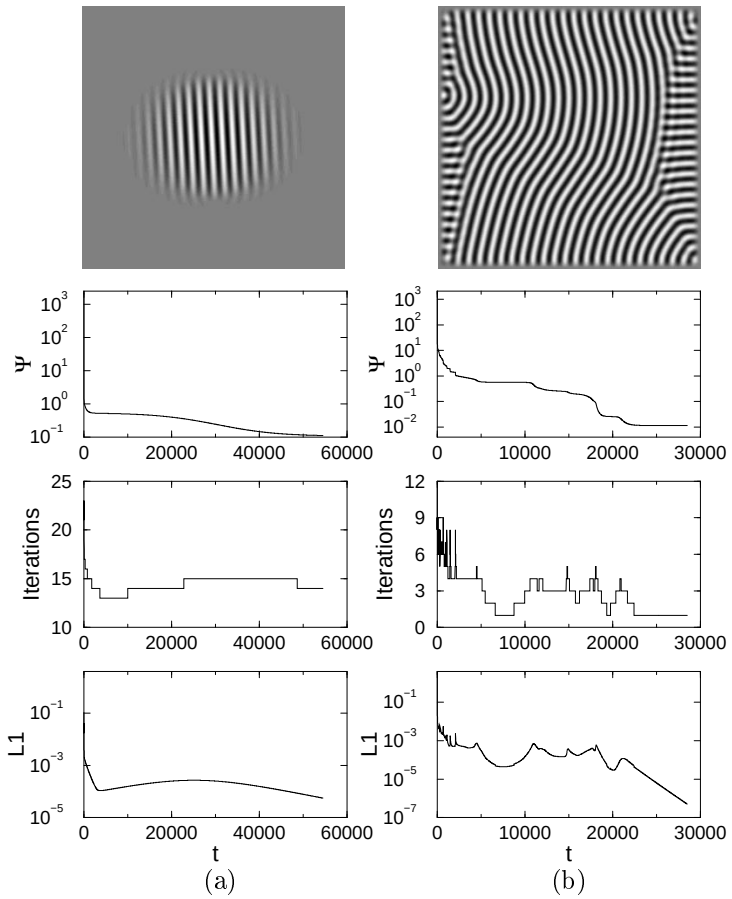


FIGURE 6.1. *Results obtained in a simulation run in a* $30 \times 30$ *box with a gaussian distribution of the bifurcation parameter across the box (a) and in a* $50 \times 50$ *box uniformly forced (case b). In the first case* $\varepsilon = 0.8\exp(-r^2/0.5) - 0.5$, *where* $r$ *is the distance from the center of the box. In case* $(b)$ $\varepsilon = 0.5$ *across the box. This figure shows the steady-state patterns, the time evolution of the associated Lyapunov finctional, the number of internal iterations accoplished in each time step and time evolution of* $L_1$. *Specified precision for the internal iterations:* $10^{-12}$ $(a)$ *and* $10^{-6}$ $(b)$. *Case* $(a)$ *was run in a P-III-600 and case* $(b)$ *was run in a IBM SP2 RISC 6000. In both cases the random initial condition was generated using the* random *function and seed 123456.*

**7. Acknowledgements.** The work of C.I.C. is supported in part by Grant LEQSF(1999-2002)-RD-A-49 from the Louisiana Board of Regents. J. P. acknowledges financial support from CNPq (Brazil) through grant No. 452399/00-9(NV). Part of the simullations was performed in the IBM SP2 RS-6000 of the NACAD-UFRJ Computer Center at the Federal University of Rio de Janeiro, Brazil.

REFERENCES

CHRISTOV, C. I., AND PONTES, J. A second-order scheme for evolution equations modelling Bénard convection. In *Proceedings of the* $8^{th}$ *Brazilian Congress of Thermal Engineering and Sciences* (Brazil, 2000). Paper S06P01 (CD).

CHRISTOV, C. I., AND PONTES, J. Numerical scheme for Swift-Hohenberg eqaution with strict implementation of the Lyapunov functional. *Mathematical and Computer Modelling* (to appear).

CHRISTOV, C. I., PONTES, J., WALGRAEF, D., AND VELARDE, M. G. Implicit time splitting for fourth-order parabolic equations. *Comput. Methods Apll. Mech. Engrg 148* (1997), 209–224.

DOUGLASS, J., AND RACHFORD, H. H. On the numerical solution of heat conduction problems in two and three space variables. *Trans. Amer. Math. Soc. 82* (1956), 421–439.

IVONIN, I. A., PAVLENKO, V. P., AND PERSSON, H. Self-consistent turbulence in the two-dimensional nonlinear Schodinger equation with a repulsive potential. *Phys. Rev. E 60* (1999), 492–499.

SWIFT, J., AND HOHENBERG, P. C. Hydrodynamic fluctuations at the convective instability. *Phys. Rev. A 15* (1977), 319–328.

YANENKO, N. N. *Method of Fractional Steps.* Gordon and Breach, NY, 1971.